Fermilab FERMILAB-Conf-03/309-E October 2003

First Run II B Physics Results From the Tevatron

Craig Blocker
Physics Department MS057
Brandeis University
415 South St.
Waltham, MA 10886, USA
Representing the CDF Collaboration

The current status of Run II at the Tevatron is covered. Upgrades of both the CDF and D0 detectors are presented, along with many illustrations of the performance and potential for significant physics measurements.

1 Introduction

The Tevatron is a copious source of B hadrons with a production cross-section four orders of magnitude greater than that at B factories. However, this is still much smaller than the total $\overline{p}p$ cross-seciton, making the the backgrounds large. Effective triggers and quality detectors are essential to extracting results.

The Tevatron is currently a unique source of B_s mesons, B_c mesons, and B baryons. Few properties of these hadrons are well measured. CDF and D0 are in a position to remedy this in the near future.

For Run II, the Tevatron was upgraded to increase the luminosity. Both the CDF and D0 detectors were upgraded to take take advantage of this increase for B physics studies, as well as other physics. This note describes the current status of the Tevatron, CDF, and D0. Also, preliminary results are presented to illustrate the potential for significant contributions to charm and bottom physics from Run II at the Tevatron.

2 Tevatron Performance

2.1 Tevatron in Run II

In 1996, the Tevatron was shutdown for installation of the Main Injector. In summer, 2001, the Tevatron began delivering beam for Run II.

For Run II, the beam energy is 980 GeV (compared to 900 GeV in Run I). The number of bunches has been increased to 36 proton bunches colliding with 36 antiproton bunches, giving a bunch crossing time of 396 ns. Originally it was planned to further increase the number of bunches and hence reduce the bunch crossing time to 132 ns. This latter upgrade has been indefinitely postponed.

At the Tevatron, the interaction region is approximately 30 cm long, necessitating long vertex detectors. On the other had, the tranverse size of the beams is about 30 μm, which is small compared to typical B hadron decay lengths of about 450 μm, allowing precision lifetime determinations.

2.2 Luminosity

Figure 1 shows the integrated and instantaneous luminosity histories for Run II. The instantaneous luminosity has been rising over the course of the run, reaching a highest value of 4.7×10^{31} cm^{2}s^{-1} as of June 1, 2003. This is still a factor of two below the nominal luminosity planned for Run IIa. This is due to a large number of small problems that will require time to remedy.

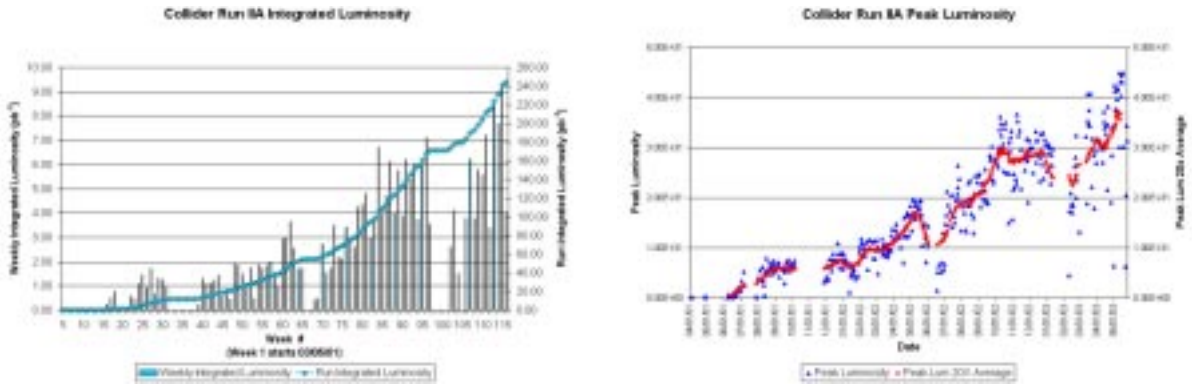

Figure 1: The integrated and instantaneous Tevatron Run II luminosities to date.

3 CDF In Run II

The CDF detector [1] was significantly upgraded for Run II and is now known as CDFII (figure 2(a)). The primary improvements were (1) a new endplug calorimeter, (2) moving the forward muon detector closer to the central detector, (3) a new silicon vertex detector, (4) a new central drift chamber, (5) a new time-of-flight system surrounding the central tracker, (6) new front-end, DAQ, and trigger electronics for the higher rates of Run II, and (7) a new trigger based on displaced tracks (tracks with non-zero impact parameter with respect to the beams).

All of these upgrades improve CDF's B physics capabilities, but the ones with the greatest impact are the silicon vertex detector and the displaced track triggers [3]. The new vertex detector is longer and has more layers than the one for Run I, increasing the fraction of tracks that have useful vertex detector information. In addition, the innermost layer is much closer to the beams, which significantly improves the decay length determination. This will be particularly important for measurements involving B_s oscillations.

The displaced track trigger is already impacting charm and B physics in CDF. In Level 1 of this trigger, the fast track processor identifies high p_T tracks using axial hits in the drift

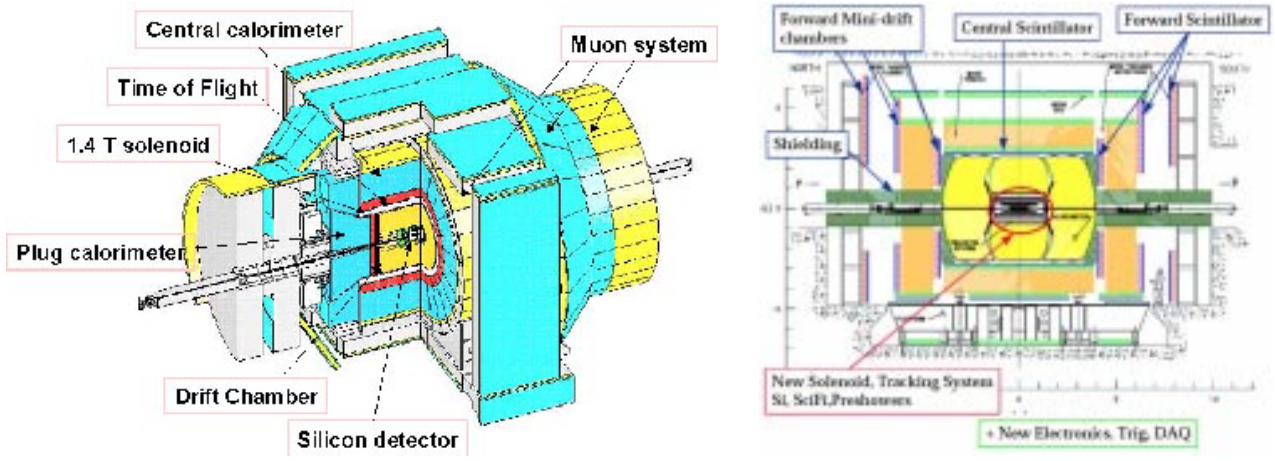

Figure 2: The (a) CDF and (b) D0 Run II detectors.

chamber tracker. At Level 2, the Secondary Vertex Trigger (SVT) matches these tracks with axial hits in the silicon vertex detector and identifies those tracks with large impact parameter d_0 with respect to the beam line. Figure 3(a) shows a distribution of the impact parameter determined online by the SVT. The 48 μm resolution includes the 33 μm transverse width of the beams.

Currently, there are two general forms of the displaced track trigger implemented. Both triggers define a displaced track as one with p_T greater than 2 GeV/c and an impact parameter greater than 100 μm. The first requires a lepton (electron or muon) along with a displaced track. The second one requires two displaced tracks. The two displaced track trigger has two subtypes. The first is designed to identify $B \to h^+h^-$ events and includes an invariant mass requirement in order to reduce the backgrounds. The second subtype is aimed at multibody B decays (such as, the very important $B_s \to D_s\pi$, which will be crucial to observation of B_s oscillations). For the second subtype, additional kinematic requirements are imposed to reduce backgrounds.

4 D0 In Run II

The D0 detector [2] (figure 2(b)) was also significantly upgraded for Run II. The major improvements were (1) a new 2 Tesla solenoidal magnet, (2) a new scintillating fiber tracker, (3) a new silicon vertex detector, (4) preshower detectors, (5) forward muon detector, (6) forward proton detector, (7) and new front-end, DAQ, and trigger electronics for the higher rates of Run II.

The B physics capabilities of D0 are greatly enhanced by the addition of the magnetic tracker system. This enables reconstruction of exclusive decay modes.

The D0 trigger system was upgraded to increase the acceptable trigger rate. In addtion, integration of tracker and silicon based triggers is underway. As with CDF, the data taking efficiency of the D0 detector has risen steadily as the detector has been commissioned during

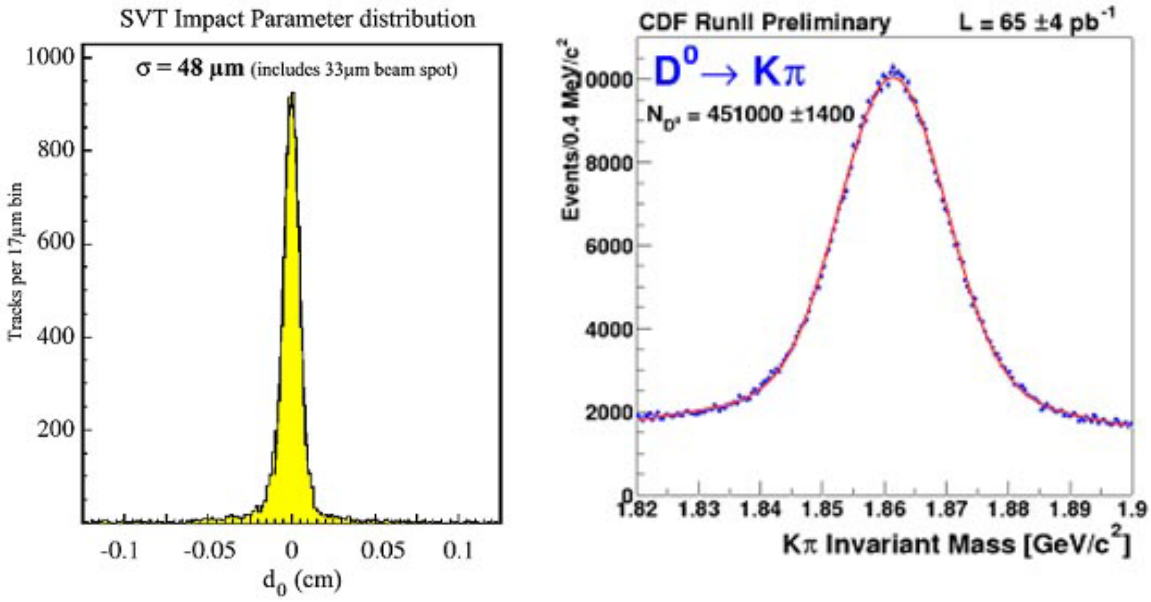

Figure 3: (a) Distribution of track impact parameters d_0 obtained online by the SVT in CDF. The 48 μm resolution includes the 33 μm width of the beams. (b) $D^0 \to K\pi$ decays from the two displaced tracks trigger in CDF.

Run II and now averages about 85%.

5 Charm Results

Although the CDF two displaced track trigger was designed for capturing hadronic B decays, it has also been very successful at triggering on charm hadron decays. For example, figure 3(b) shows a sample of 451,000 $D^0 \to K^-\pi^+$ decays [4] from 65 pb^{-1} of data.

First charm physics results are already coming out of CDFII. Figure 4 shows signals for the decay $D^{*+} \to D^0\pi^+$ followed by the decays $D^0 \to K^+K^-$, $K^-\pi^+$, and $\pi^+\pi^-$. From these, the relative partial widths are determined to be , $(D^0 \to K^+K^-)/$, $(D^0 \to K^-\pi^+) = (9.38 \pm 0.18 \pm 0.10)\%$ and , $(D^0 \to \pi^+\pi^-)/$, $(D^0 \to K^-\pi^+) = (3.686 \pm 0.076 \pm 0.036)\%$. These values are in agreement with the current Particle Data Group (PDG) ones, but already have smaller uncertainties.

In these events, the charge of the soft pion from the D^* decay tags whether it is a D^0 or a $\overline{D}^0$, allowing a determination of the direction CP asymmetry A_{CP} in these decays to be

$$A_{CP}^{KK} = (2.0 \pm 1.7 \pm 0.6)\% \quad (1)$$

$$A_{CP}^{\pi\pi} = (3.0 \pm 1.9 \pm 0.6)\%, \quad (2)$$

where A_{CP} is defined as

$$A_{CP} = \frac{, (D^0 \to f) - , (\overline{D}^0 \to f)}{, (D^0 \to f) + , (\overline{D}^0 \to f)}, \quad (3)$$

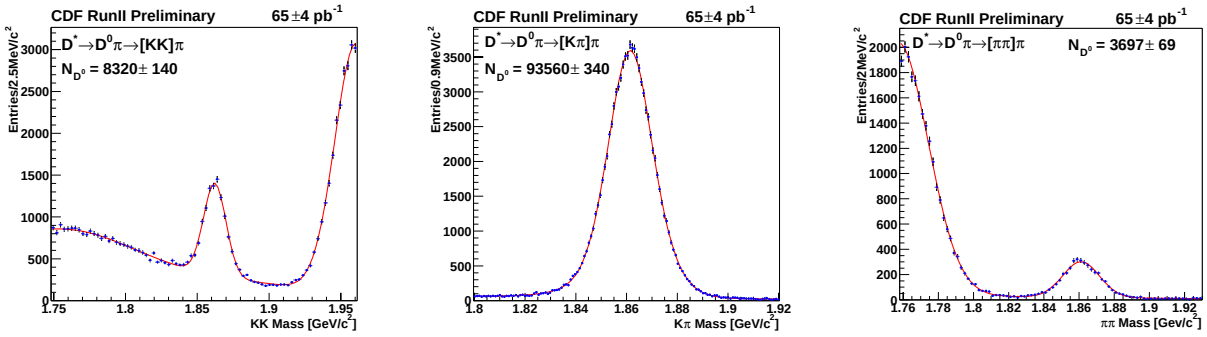

Figure 4: $D^{*+} \to D^0\pi^+, D^0 \to$ (a) K^+K^-, (b) $K^-\pi^+$, and (c) $\pi^+\pi^-$ decays in CDF.

for final state f. For A_{CP}, the uncertainties are comparable to current PDG values.

CDF has also searched for the rare decay $D^0 \to \mu^+\mu^-$ and has found no candidates (figure 5(a)). The kinematically nearly identical $D^0 \to \pi^+\pi^-$ events (figure 4(c)) are used for normalization, resulting in an upper limit on the branching ratio of 2.4×10^{-6} at the 90% confidence level.

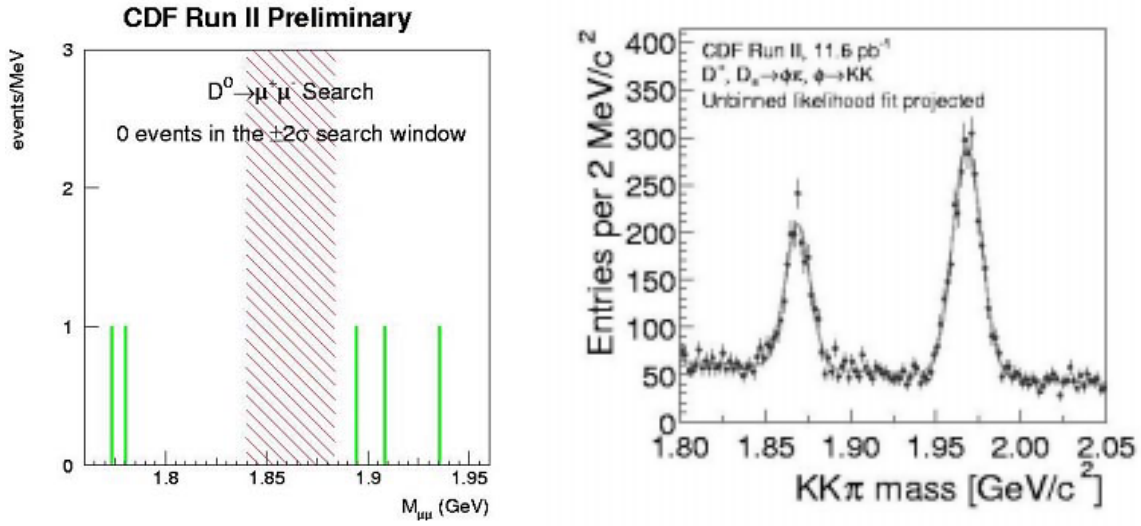

Figure 5: (a) Search for $D^0 \to \mu^+\mu^-$ in CDF data. No candidate events are seen. (b) Invariant mass of $\phi\pi$ events at CDF showing the D^+ and D_s. These events are used to determine the D_s–D^+ mass difference.

The first CDF Run II publication has been submitted on the mass difference between the D_s and D^+. These are observed in the same decay mode $D \to \phi\pi^\pm \to K^+K^-\pi^\pm$ (figure 5(b)), which means that most of the systematic uncertainties cancel. The mass difference is $m(D_s) - m(D^+) = 99.41 \pm 0.38 \pm 0.21$ GeV/c^2, which agrees with the PDG value and has comparable uncertainty. This measurement (along with the other plots in this paper) illustrate the excellent mass resolution of CDF and that the mass scale is well understood in Run II.

6 B Results

6.1 J/ψ Modes

As in Run I, CDF and D0 both have triggers that identify $J/\psi \to \mu^+\mu^-$ decays. These J/ψ's can then be used to find and study B's. For example, figure 6 shows samples of $B_d \to J/\psi K_s$ and $B_d \to J/\psi K^{*0}$ from D0. See Vivek Jain's talk in these proceedings [5] for a discussion of lifetime measurements extracted by D0 and CDF from these and similar decay modes.

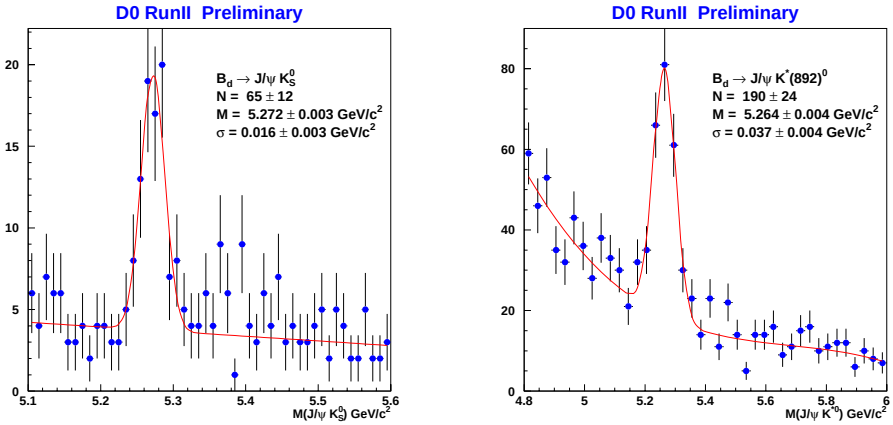

Figure 6: (a) $B_d \to J/\psi K_s$ and (b) $B_d \to J/\psi K^{*0}$ decays in D0.

CDF has used similar decays (figure 7) to make preliminary Run II measurements of the B meson masses, giving $m(B_s) = 5365.50 \pm 1.26 \pm 0.94$ MeV/c^2, $m(B^+) = 5279.32 \pm 0.68 \pm 0.94$ MeV/c^2, and $m(B^0) = 5280.30 \pm 0.92 \pm 0.94$ MeV/c^2. The values are in agreement with the PDG values. The uncertainties, particularly for the B^+ and B^0 are somewhat larger than the PDG values but will be reduced with more data.

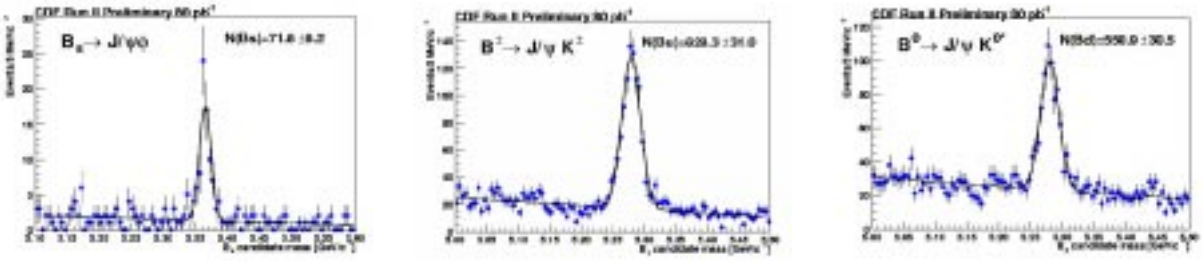

Figure 7: $B_s \to (a)J/\psi\phi$, (b) $B^+ J/\psi K$, and (c) $B^0 \to K^{0*}$ decays in CDF.

6.2 Hadronic Modes

Figure 8(a) shows the h^+h^- (here, h stands for hadron, namely $K^\pm$ or $\pi^\pm$) invariant mass of pairs of tracks that satisfy the CDF two displaced tracks trigger (after additional cuts to enhance the signal to background). A clear B signal is seen, which is a combination of $B_d \to \pi^+\pi^-$, $B_d \to K^+\pi^-$, $B_s \to K^+K^-$, and $B_s \to K^-\pi^+$. CDF does not have sufficient particle identification to separate these decays on an event–by–event basis, but by using the available dE/dx along with the excellent mass resolution and other kinematical variables, a statistical separation is possible. For more details, see reference [6]. Eventually with sufficient statistics, CDF will measure the CP violating asymmetries in these decays. From these, the CKM angle γ can be extracted.

Figure 8(b) shows a sample from CDF of $B_s \to \overline{D}_s\pi^+$, $\overline{D}_s \to \phi\pi^-$ decays, illustrating the power of the multibody two displaced track trigger. This is the golden mode for observing B_s oscillations. The wide peak on the left is a reflection from the decay $B_s \to \overline{D}_s^*\pi^+$, where the γ from the $\overline{D}_s^*$ decay is not observed. These decays can also be used for studying B_s oscillations. Note that about 1000 events are needed to observe B_s oscillations at the five standard deviation level if Δm_s has the value expected in the Standard Model.

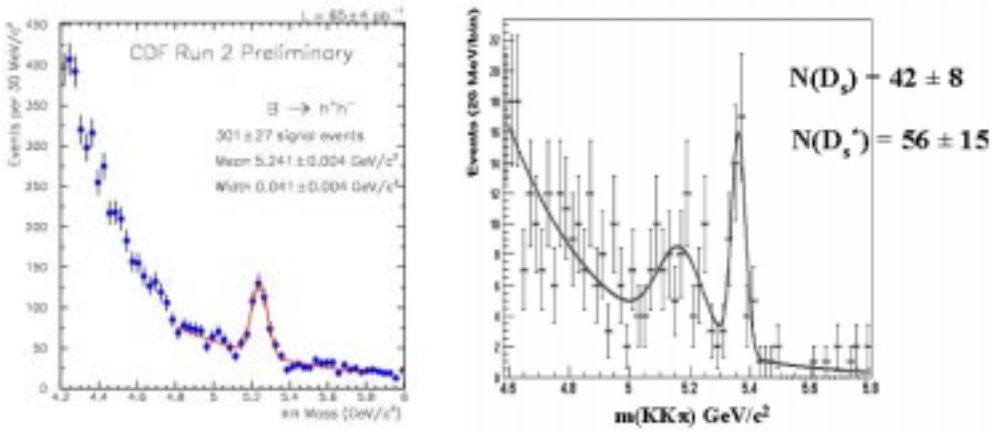

Figure 8: B signals from the CDF two displaced track trigger. (a) $B \to h^+h^-$ and (b) $B_s \to \overline{D}_s\pi^+$, $\overline{D}_s \to \phi\pi^-$.

Figure 9(a) shows a sample of $\Lambda_b \to \Lambda_c\pi^-$, $\Lambda_c \to pK^-\pi^+$ from CDF, illustrating the ability to identify B baryons. More details on this decay mode can be found in Mat Martin's contribution to these proceedings [6].

A sample of $B^+ \to \phi K^+$ events from CDF is shown in figure 9(b), showing that CDF can find relatively rare modes with manageable background levels.

7 Conclusions

Run II at the Tevatron is underway. Although the luminosity has been lower than hoped, it is increasing. The CDF and D0 detectors are both functioning well and taking data at

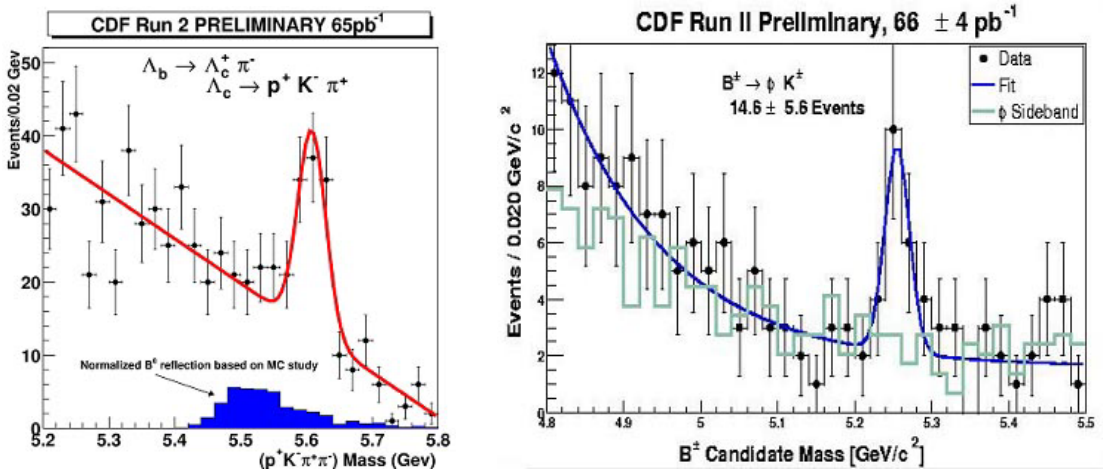

Figure 9: (a) $\Lambda_b \to \Lambda_c \pi^-$, $\Lambda_c \to pK^-\pi^+$ events and (b) $B^+ \to \phi K^+$ events from CDF.

high efficiency. Detector upgrades have significantly enhanced the B physics potential of both detectors, with new results on charm and bottom physics already coming out and with the promise of many more interesting observations in the near future.

Acknowledgments

For all my colleagues, I express our appreciation for the work of all CDF and D0 collaborators, those who work on the Tevatron, and all of the funding agencies that support this work. In addition, I thank the organizers and staff of FPCP2003 for a very enjoyable conference.

References

[1] CDF II Collaboration, Fermilab-PUB96/390-E (1996)

[2] D0 Collaboration, Fermilb-PUB96/357-E (1996)

[3] W. Ashmanskas *et al.*, Nucl. Intr. Meth. **A447**, 218 (2000)

[4] The charge conjugate reaction is also implied for all decays in this paper.

[5] V. Jain, "B Lifetimes and $B\overline{B}$ mixing", *these proceedings pp.* **??-??**

[6] M. Martin, "Branching Ratios from B_s^0 and Λ_B^0", *these proceedings pp.* **??-??**